Title: Three-dimensional characterization of medium spiny neuron heterogeneity in the adult mouse striatum

Authors: Jenesis Gayden[1,2], Stephanie Puig[3], Chaitanya Srinivasan[4], Silas A. Buck[1,2], Mackenzie C. Gamble[3,5], Jill R. Glausier[2], Hugo A. Tejeda[6], Yan Dong[2,7], Andreas R. Pfenning[4,8], Ryan W. Logan[9], Zachary Freyberg[2,10*]

[1]Center for Neuroscience, University of Pittsburgh, Pittsburgh, PA, USA
[2]Department of Psychiatry, University of Pittsburgh, Pittsburgh, PA, USA
[3]Department of Pharmacology and Experimental Therapeutics, Boston University School of Medicine, Boston, MA, USA
[4]Department of Computational Biology, Carnegie Mellon University, Pittsburgh, PA, USA
[5]Molecular and Translational Medicine, Department of Medicine, Boston University School of Medicine, Boston, MA, USA
[6]Unit on Neuromodulation and Synaptic Integration, National Institute of Mental Health, National Institutes of Health, Bethesda, MD, USA
[7]Department of Neuroscience, University of Pittsburgh, Pittsburgh, PA, USA
[8]Neuroscience Institute, Carnegie Mellon University, Pittsburgh, PA, USA
[9]Department of Psychiatry, University of Massachusetts Chan Medical School, Worcester, MA, USA
[10]Department of Cell Biology, University of Pittsburgh, Pittsburgh, PA, USA

*Corresponding author:
Zachary Freyberg, M.D., Ph.D.
3811 O'Hara Street, BST W1640
Pittsburgh, PA 15213
Tel: (412) 648-0033
Email: freyberg@pitt.edu

Abstract

Striatal dopamine (DA) neurotransmission is critical for an array of reward-related behaviors and goal-directed motor control. In rodents, 95% of striatal neurons are GABAergic medium spiny neurons (MSNs) that have been traditionally segregated into two subpopulations based on the expression of stimulatory DA D_1-like receptors versus inhibitory D_2-like receptors. However, emerging evidence suggests that striatal cell composition is anatomically and functionally more heterogenous than previously appreciated. The presence of MSNs that co-express multiple DA receptors offers a means to more accurately understand this heterogeneity. To dissect the precise nature of MSN heterogeneity, here we used multiplex RNAscope to identify expression of three predominantly expressed DA receptors in the striatum: DA D_1 (D1R), D_2 (D2R), and D_3 (D3R) receptors. We report heterogenous subpopulations of MSNs that are distinctly distributed across the dorsal-ventral and rostral-caudal axes of the adult mouse striatum. These subpopulations include MSNs that co-express D1R and D2R (D1/2R), D1R and D3R (D1/3R), and D2R and D3R (D2/3R). Overall, our characterization of distinct MSN subpopulations informs our understanding of region-specific striatal cell heterogeneity.

Introduction

The striatum is a critical nexus for motivational regulation and motor control. Critically, dopamine (DA) signaling is important for striatal function and its dysfunction is strongly associated with disorders from schizophrenia and substance use disorders to Parkinson's disease (PD). 95% of striatal neurons consist of GABAergic medium spiny neurons (MSNs) that have traditionally been segregated into two subpopulations based on expression of DA D_1-like versus D_2-like receptors[1-3]. D_1-like receptors include DA D_1 and D_5 receptors (D1R, D5R) and D_2-like receptors include DA D_2, D_3, and D_4 receptors (D2R, D3R, D4R). There is extensive evidence showing that the expression of D_1-like versus D_2-like receptors confers different properties at cellular, circuit, and behavioral levels[4-9].

At the cellular level, D_1-like and D_2-like receptors are coupled to different G proteins, resulting in different cellular properties[3, 10]. These signaling differences between $D1R^+$ versus $D2R^+$ MSNs extend to differences in neuronal activity and electrophysiological properties[11-14]. In fact, $D2R^+$ MSNs exhibit increased excitability and higher spontaneous excitatory postsynaptic currents compared to $D1R^+$ MSNs[4]. For example, in the nucleus accumbens (NAc) region of the striatum, a key difference between $D1R^+$ and $D2R^+$ MSNs is that $D1R^+$ MSNs preferentially project to the ventral tegmental area, while $D2R^+$ MSNs primarily project to the ventral pallidum[15]. Consequently, $D1R^+$ versus $D2R^+$ NAc MSNs contribute to distinct and, on many occasions, opposing motivated behaviors including those relevant to reward- and addiction-related behaviors[16-19]. Importantly, manipulations of these NAc $D1R^+$ or $D2R^+$ MSNs alone cannot recapitulate the full range of striatal behaviors[20]. This suggests that the composition of MSNs is more heterogenous than previously thought[7, 12, 13], with additional MSN subpopulations that contribute to these behaviors.

Within $D1R^+$ and $D2R^+$ MSN subpopulations, electrophysiological response properties are not uniform. In fact, measures of the strength and release probability of glutamatergic synapses show a biphasic heterogeneity between $D1R^+$ and $D2R^+$ populations[12]. In the context of drugs of abuse, the differences in $D1R^+$ versus $D2R^+$ MSNs also translate to addiction-related behaviors including drug-induced conditioned place preference[21, 22]. Collectively, these data suggest additional striatal MSN subpopulations apart from the MSNs that solely express either D1R or D2R. Consistent with this, recent work found evidence of MSNs that express both receptors[23-26]. Yet, the physiological relevance of D1R and D2R co-expression remains controversial. Some studies point to D1R and D2R forming higher order complexes that confer signaling process distinct from either D1R or

D2R alone[27, 28]. Alternatively, others suggest that these receptors may operate independently of one another in co-expressing cells[29]. Despite these differing viewpoints, we posit that MSNs co-expressing D1R and D2R may confer unique circuit and signaling properties, irrespectively of whether the receptors form heteromeric complexes or not. This raises the possibility of anatomically and functionally distinct striatal MSN subpopulations.

Compared to D1R and D2R, considerably less is known about the biology and anatomic distribution of D3R. Early autoradiographic studies revealed that D3R is present in the striatum, predominantly expressed in the core and shell subregions of the NAc and the Islands of Calleja (IC)[30]. Increasing evidence suggests that, like D1R and D2R, D3R is also critical for striatal function. Recent studies demonstrate the importance of D3R signaling in the IC for rodent grooming behavior[31]. Furthermore, striatal D3R signaling is implicated in disease states including PD dyskinesia and in conditioning to drugs of abuse[32]. Similar to D1R and D2R, D3R may similarly interact with other DA receptors. Indeed, D1R and D3R have been shown to form heteromeric complexes *in vitro* via heterologous overexpression[33, 34]. This raises an even more fundamental question: is D3R co-expressed with D1R in the same cells endogenously in striatum? Determining D3R's expression patterns is a necessary step in better understanding its physiological relevance.

Historically, studying striatal DA receptor expression has been limited by the lack of specific antibodies, as well as spatial resolution below the single-cell level using earlier methods such as autoradiography[35]. The recent development of significantly more sensitive, quantitative approaches with single-cell resolution such as multiplex RNAscope, a form of fluorescent *in situ* mRNA hybridization, has been instrumental in overcoming these limitations. RNAscope enabled us to quantitatively dissect the expression of DA receptors on a cell-by-cell basis throughout the striatum. Our present study establishes a definitive three-dimensional (3D) map of D1R, D2R, and D3R mRNA expression in mouse striatum. We confirm co-expressing MSN subpopulations (D1/2R, D1/3R, D2/3R) that are discrete from MSNs that solely express D1R, D2R, or D3R. Importantly, we reveal that these populations have distinct spatial distributions, not only in the dorsal-ventral direction, but also along a rostral-caudal axis. These differences in distribution point to a 3D gradient of DA receptor expression in adult mouse brain.

Methods

Animals

Adult male and female C57BL/6J mice from The Jackson Laboratory (stock 000664, 8-14-wks-old; Bar Harbor, ME) were used for this study. All animals were group-housed in a 12/12 light cycle with water and rodent chow provided *ad libitum*. All procedures were performed in compliance with the Institutional Animal Care and Use Committee at the University of Pittsburgh (protocol #22071493).

Brain tissue preparation

Mice were euthanized by rapid cervical dislocation performed by an experienced experimenter. Brains were collected and snap-frozen in isopentane at -55°C, then stored at -80°C until use. Brains were sectioned using a cryostat at -18°C. 14μm sections were collected at bregma -1.61mm (termed Rostral 1), bregma -1.33mm (termed Rostral 2), bregma -1.15mm (termed Rostral 3), bregma +0.91mm (termed Caudal) (Figure 1). Following mounting on slides (Superfrost+, Fisher Scientific, Waltham, MA), samples were first dried at -20°C for 2h, followed by additional drying at -80°C overnight.

Multiplex fluorescent *in situ* hybridization

Multiplex RNAscope technology (ACDBio, Neward, CA) was used to profile mRNA expression of Drd1a, Drd2, and Drd3 genes. RNAscope labelling of fresh frozen brain tissue was conducted according to manufacturer instructions using the ACD Bio RNAscope v1 kit. Briefly, pre-mounted tissue sections were post-fixed on slides in pre-chilled 4% paraformaldehyde (4°C, 60 min). Tissue underwent dehydration in successive ethanol baths of increasing concentration (50%, 70%, 100%). After drying, a hydrophobic barrier was drawn around samples, followed by incubation with probes (2h, 40°C) to detect cell-specific expression of mouse Drd1a (ACD Bio, Mm-Drd1a, Cat. 406491), Drd2 (Mm-Drd2-C2, Cat. 406501-C2), and Drd3 (Mm-Drd3-C3, Cat. 447721-C3). Following hybridization, slides underwent signal amplification with the respective probes allocated to each channel labeled with the following fluorophores: Channel 1, Atto 550; Channel 2, Alexa fluor 647; Channel 3, Alexa fluor 488. Tissue was then counter-stained with DAPI to label cell nuclei and mounted with Vectashield (Vector Labs, Neward, CA). Slides were stored at 4°C until imaging.

To test signal specificity of the RNAscope probes in our striatal tissue samples, we used RNAscope 3-plex Positive Control Probe (ACD Bio, Cat. 320881) and 3-plex Negative Control Probe (ACD Bio, Cat. 320871). Tissue preparation, hybridization, and signal amplification were as described above. The species-specific 3-plex Positive Control Probe labeled housekeeping

gene controls for all 3 channels: Channel 1: DNA-directed RNA polymerase II subunit RPB1 (POL2RA); Channel 2: Cyclophilin B (PPIB); and Channel 3: Ubiquitin C (UBC)(Fig. S1A, B). The universal 3-plex Negative Control Probe contained probes targeting the DapB gene for all 3 channels (Fig. S1C, D).

Fluorescence slide scanning microscopy

Fluorescence imaging of labeled slides was performed using the Olympus VS200 automated slide scanner (Olympus, Center Valley, PA). Exposure times were adjusted for each fluorophore to ensure proper signal distribution with no signal saturation. Coronal sections were identified by experimenters and Z stacks of 3μm (3 Z-planes spaced by 1μm each) were imaged using a dry 20X objective lens (N.A. 0.8). Identical exposure settings and magnifications were consistently applied to all slides. After image acquisition, Z stacks were converted to two-dimensional maximum intensity projections and deconvolved using NIS Elements software (Nikon, Melleville, NY).

Image analysis

Image analysis was performed using the HALO image analysis platform equipped with a fluorescent *in situ* hybridization plug-in (Version 3.0, Indica Labs, Albuquerque, NM). Nuclei were quantified as DAPI-stained objects with the minimum cytoplasmic radius set at 5μm. Puncta corresponding to the respective mRNA probes were quantified as any 0.03-0.15μm^2 object. We established a methodology to define cells specifically labelled by the respective probes above non-specific background. 1) We normalized the number of puncta per probe by dividing by the number of mRNA grains by total area analyzed (grains/area analyzed). 2) We then tested thresholds of 3x, 5x, 7x, and 10x above the puncta/area analyzed values based on our earlier RNAscope studies[36]. Examining the grains/area analyzed at 7-fold above the baseline (7x threshold) best optimized signal-to-noise in our datasets, providing accurate identification of appropriately labelled cells while minimizing non-specific signal. 3) We quantified the number of cells that reached this 7x threshold for each respective probe in a given sample. 4) To calculate the cellular density of positive cells, we divided the number of positive cells by the total area analyzed and converted to mm^2 units.

To generate heat maps showing distribution of cells positive for single or double expression of dopamine receptors, images were analyzed using the spatial analysis module on the HALO

platform. The previously described thresholds were also applied to account for background in the heat maps.

Statistical analyses

GraphPad Prism (version 9.20, San Diego, CA) and SPSS (Version 28.01.1, IBM, Armonk, NY) were used for all statistical analyses. One-way ANOVA followed by Tukey's multiple comparison tests were employed to analyze differences in the density of positive cells across striatal subregions. Three-way ANOVA, followed by Tukey's post hoc comparisons, identified potential interactions between DA receptor expression, striatal subregion, and position along the rostral-caudal axis.

Results

Establishing RNAscope mapping of mouse striatum

We comprehensively examined the mRNA expression of D1R, D2R, and D3R, three predominantly expressed striatal DA receptors, across entire striatal brain slices of adult mouse striatum via multiplex RNAscope. This enabled us to quantify expression of D1R, D2R, and D3R in key striatal structures: the caudate putamen (CPu), the NAc core (Core), the NAc shell (Shell), and the olfactory tubercle (OT) (Fig. 1). Moreover, we confirmed the specificity of the RNAscope approach in mouse striatum by testing pre-validated positive and negative controls (Supplementary Fig. S1).

Spatial distribution of striatal Dopamine D_1, D_2, D_3 receptor expression in singly-expressing medium spiny neurons

We confirmed expression of D1R, D2R, and D3R throughout the striatum along both dorsal-ventral and rostral-caudal axes. We identified discrete populations of MSNs that either express a single DA receptor subtype (D1R-only, D2R-only, or D3R-only) (Fig. 2, Supplementary Fig. S2) versus MSNs that co-express multiple receptor subtypes (D1/2R, D1/3R, D2/3R) (Fig. 3, Supplementary Fig. S3). Focusing on MSNs expressing only one DA receptor subtype (Fig. 2), there was a significant interaction between cell type, striatal subregion, and position along the rostral-caudal axis [$F(17,790)=1.68$, $p=0.042$]. Since we found no differences in cell densities of all MSN subpopulations tested according to sex ($p>0.05$), we combined both sexes in subsequent analyses.

D1R-only MSNs. D1R was robustly expressed throughout the striatum, which was especially evident in the extensive distribution of MSNs that solely express this receptor (D1R-only; Fig. 2A). We additionally discovered distinct patterns of D1R expression across both dorsal-ventral and rostral-caudal axes. Beginning in the most rostral section (Rostral 1), the density of D1R-only cells was greatest in the OT (Fig. 2B) compared to the other striatal subregions [$F(3,58) = 6.24$, $p=0.001$]. Closer analysis of the individual subsections of the Shell (*e.g.*, medial, ventral, and lateral shell subsections; Fig. 1 inset) revealed that the differences in D1R-only cell density between the OT and Shell in the Rostral 1 section were primarily driven by the lateral NAc shell ($p=0.016$; Supplementary Fig. S2A). Moving caudally, significant differences in D1R-only cell density between the OT and other striatal subregions gradually diminished and ultimately disappeared by Rostral 3 and Caudal sections ($p>0.05$; Fig. 2C-E).

D2R-only MSNs. Consistent with earlier work, D2R is widely expressed in the striatum and, similar to D1R-only cells, we identified MSNs that only express D2R (D2R-only; Fig. 2F). In the Rostral 1 section, we observed an overall significant difference in the distribution of D2R-only cells across the striatal subregions ([$F(3,56) = 4.25$, $p=0.009$]; Fig. 2F-J). There is a significantly lower density of D2R-only cells in the OT compared to the Shell ($p=0.005$; Fig. 2G). This is due to differences in D2R-only cell density specific to the medial NAc shell ($p<0.0001$; Supplementary Fig. S2E). Interestingly, moving caudally reveals trends in cell distribution that are the opposite to those of D1R-only MSNs. Specifically, moving caudally, D2R-only cell density decreases in the OT [$F(3,41) = 3.88$, $p=0.02$], Shell [$F(3,133) = 24.23$, $p=<0.0001$], and Core [$F(3,37) = 8.09$, $p=0.0003$). In contrast, CPu D2R-only cell density increases from Rostral 1 to Rostral 2 ($p=0.014$) and remains stable throughout the remainder of the rostral-caudal axis (Fig. 2I, J).

D3R-only MSNs. We observed a distinct subpopulation of striatal D3R-only MSNs, albeit in far smaller numbers compared to D1R-only and D2R-only cells (Fig. 2L-O). The representative heat map analysis revealed small, dense pockets of D3R-only cells concentrated in the Shell and the OT, primarily within the IC (Fig. 2K). Unlike D1R- and D2R-only cells, we observed no differences in striatal distribution of D3R-only MSNs across either the dorsal-ventral or rostral-caudal axes ($p>0.05$; Fig. 2L-O, Supplementary Fig. S2I-L).

Spatial distribution of striatal Dopamine D_1, D_2, D_3 receptor expression in co-expressing medium spiny neurons

Our multiplex RNAscope studies also revealed several distinct striatal MSN subpopulations that co-express either D_1 and D_2 DA receptors (D1/2R), D_1 and D_3 DA receptors (D1/3R), or D_2 and D_3 DA receptors (D2/3R)(Fig. 3, Supplementary Fig. S3). We found no evidence of MSNs that co-expressed all three DA receptors together, *i.e.*, D1/2/3R. Threshold analyses ensured we did not double count cells (see Methods), enabling us to accurately distinguish MSNs that only express a single DA receptor from MSNs co-expressing multiple DA receptors. Quantification revealed that, while DA receptor co-expressing MSNs are clearly present throughout striatum, these cells are found in markedly lower numbers compared to MSNs that express single DA receptors. Interestingly, our analyses also demonstrated additional dorsal-ventral and rostral-caudal trends in cell distribution for the co-expressing neurons (Fig. 3).

D1/2R MSNs. Quantification showed that D1/2R MSNs constitute approximately 10-25% of the total pool of $D1R^+$ and $D2R^+$ cells in striatum (Table 1). Of these co-expressing cells, there is significant enrichment in the OT that persists throughout the rostral-caudal axis. In more rostral sections (Rostral 1-3), the OT possesses as much as double the D1/2R MSN density compared to all other striatal subregions (Fig. 3B-D) [Rostral 1: $F(5,54) = 3.954$, $p=0.004$; Rostral 2: $F(5,65) = 4.227$, $p=0.002$; Rostral 3: $F(5,63) = 3.309$, $p=0.01$)]. Moving caudally, however, we observed a gradual decrease in the OT's enrichment in D1/2R MSNs (Fig. 3B-E). Closer inspection of the Shell subregions revealed similar trends across the rostral-caudal axis (Supplementary Fig. S3A-D).

Along the dorsal-ventral axis, we examined the relative proportion of D1/2R neurons out of the total number of MSNs that express either D1R or D2R. Our analyses confirmed the relative abundance of D1/2R MSNs in the OT compared to other striatal subregions. Indeed, OT D1/2R MSNs constitute as many as 20-28% of the total number of $D2R^+$ cells, while composing 12-16% of $D1R^+$ cells in this region (Table 1). Besides the OT, we also observed changes in other striatal subregions along the dorsal-ventral axis. For example, in the Rostral 3 section, there is a significant increase in the proportion of D1/2R MSNs in the CPu versus the Shell relative to the total number of $D1R^+$ cells ($p=0.001$). Additionally, in the most caudal section (Caudal), the proportion of Shell D1/2R MSNs relative to the total pool of $D1R^+$ cells is significantly lower compared to other subregions including the CPu ($p=0.014$), Core ($p=0.041$), or the OT ($p=0.007$).

We also find Shell-specific differences in relative densities of D1/2R MSNs along the rostral-caudal axis. Out of the total number of $D1R^+$ cells, there are significantly more Shell D1/2R MSNs

in the most rostral section (Rostral 1) compared to the most caudal section (Caudal) (p=0.011). In contrast, out of the total number of Shell D2R$^+$ cells, there is a significantly higher proportion of D1/2R MSNs in the Rostral 2 section compared to Rostral 1 (p=0.046) (Table 1). Taken together, these data point to shifts in the distributions of co-expressing D1/2R MSNs across both dorsal-ventral and rostral-caudal axes, suggesting predefined patterns of receptor expression.

D1/3R MSNs. In contrast to the relatively small numbers of D3R-only MSNs, most striatal MSNs co-express D3R alongside D1R (D1/3R MSNs). Nevertheless, compared to D1/2R MSNs, D1/3R MSNs constitute a much smaller proportion of the total D1R$^+$ MSN population, ranging from 0-7% based on the striatal subregion and position along the rostral-caudal axis (Fig. 3F-J, Table 1). Along the dorsal-ventral axis, there is OT enrichment of D1/3R MSNs in the Rostral 1 section [$F(3,58)=5.564$, p=0.002; Fig. 3G], with no further enrichment in the more caudal sections (p>0.05; Fig. 3H-J). Akin to D1/2R MSN distribution, the changes in D1/3R density along the rostral-caudal axis are exclusive to the Shell. Specifically, the proportion of Shell D1/3R MSNs out of total D1R$^+$ neurons is higher in the Rostral 1 section compared to Rostral 2 (p=0.003), Rostral 3 (p=0.001), and Caudal (p=0.004) sections (Table 1).

D2/3R MSNs. Of the three DA receptor co-expressing MSNs, D2/3R MSNs represent the smallest striatal subpopulation (Fig. 3K). Limited numbers of D2/3R cells are primarily expressed in the ventral striatum with no significant distribution in the CPu or Core. This pattern is present across all striatal sections throughout the rostral-caudal axis (Fig. 3L-O; Table 1).

Discussion

Striatal MSNs that co-express DA receptors are increasingly implicated in a variety of contexts, including reward-learning, decision-making, and goal-directed movement[37, 38]. Nevertheless, most evidence of DA receptor co-expressing MSN subpopulations has been indirect. Our use of multiplex RNAscope provides direct confirmation of multiple MSNs subpopulations in well-defined patterns. Using this approach, we have established a 3D map of DA receptor-expressing MSN subtypes in adult mouse striatum. Here, we find unique subpopulations of MSNs that co-express either D1/2R, D1/3R, or D2/3R. These co-expressing cells are heterogeneously distributed throughout the striatum along the dorsal-ventral and rostral-caudal axes.

There are well-defined relationships between striatal anatomy and function[39]. For example, functional differences have been described for distinct NAc subregions where DA transient release amplitude and frequency differ in the Core versus the Shell[40]. Regional differences in DA signaling have also been extensively documented in the context of drugs of abuse where the dorsal versus ventral striatum exhibit different molecular responses in assays of drug-seeking behavior[41,42]. Furthermore, post-cocaine DA transient releases produce distinct responses along a dorsal-ventral gradient in the striatum[40]. What signaling mechanisms can explain these differences? Traditionally, striatal DA signaling has been divided along a functional dichotomy between $D1R^+$ and $D2R^+$ MSNs. In fact, at a basal level, $D2R^+$ MSNs exhibit increased excitability and higher spontaneous excitatory postsynaptic currents compared to $D1R^+$ MSNs[4]. In the context of opioids, morphine differentially acts on $D1R^+$ versus $D2R^+$ NAc MSNs. Morphine increases glutamatergic synaptic strength in NAc $D1R^+$ MSNs, while $D2R^+$ MSNs show opposite effects[12]. Intriguingly, opioid-induced responses in $D1R^+$ and $D2R^+$ MSNs are heterogenous, raising the possibility of unique subpopulations of striatal cells. Indeed, electrophysiological differences between $D1R^+$ and $D2R^+$ MSNs are not uniform. In fact, measures of synaptic strength and glutamate release probability show a biphasic heterogeneity in both $D1R^+$ and $D2R^+$ populations[12].

Consistent with evidence of MSN heterogeneity, we hypothesized: 1) the existence of distinct subpopulations of MSNs that co-express multiple DA receptors, and 2) these co-expressing subpopulations exhibit unique anatomic distributions in striatum. Our data indeed demonstrate the existence of several MSN subpopulations that co-express either D1/2R, D1/3R, or D2/3R. Though these subpopulations constitute a minority of the total striatal MSN pool, we consistently observed DA receptor co-expression in specific striatal subregions in well-defined 3D patterns. We found that D1/2R MSNs are enriched in the OT compared to other striatal regions. Our findings corroborate and expand upon earlier work which similarly identified discrete MSN subpopulations along a dorsolateral-ventromedial gradient[43]. Using a combination of single-cell RNA sequencing and computational analysis, Stanley and colleagues focused on D1R and D2R MSNs and defined four discrete MSN subpopulations based on their transcriptional profiles and their relative striatal localizations: i) D1R-expressing MSNs, ii) D2R-expressing MSNs, iii) hybrid D1/2R MSNs, and iv) OT D1R MSNs located in the IC that are transcriptionally distinct from all other $D1R^+$ striatal cells[43].

The co-expression of different DA receptors in the same MSNs also raises a key question: does DA receptor co-expression confer unique properties compared to expression of either receptor alone? Computational models have proposed that D1/2R-co-expressing MSNs have distinct roles in reward-punishment-risk-based decision-making[37]. In the disease context, D1/2R MSNs are uniquely affected by dopaminergic deafferentation in preclinical models of PD[44]. However, the mechanisms by which D1/2R co-expression achieves these effects remain poorly understood. Earlier work suggests that co-expression of D1R and D2R leads to the formation of higher-order heteromeric complexes[45]. These D1/2R complexes may enable recruitment of downstream effector molecules (*i.e.,* $G\alpha_q$) that are different from those recruited to either D1R ($G\alpha_s$) or D2R ($G\alpha_{i/o}$) alone[46]. Functionally, D1/2R receptor heteromeric complexes have been implicated in cocaine-induced locomotion and self-administration[47]; these heteromers are also associated with anxiety-like and depressive-like behaviors[48]. Outside of the brain, D1/2R heteromers may also modulate pancreatic islet function[49]. However, the physiological relevance of DA receptors heteromers remains controversial as most of these studies relied on exogenous overexpression. This raises the possibility that D1/2R heteromers may not be relevant physiologically since endogenous levels are often far lower than the levels produced via heterologous overexpression. Indeed, other studies provide evidence against the existence of endogenously expressed D1/2R heteromers[29], suggesting that the individual classes of receptors may operate independently of one another when co-expressed in the same cells. Nevertheless, irrespective of whether D1R and D2R form heteromers or primarily function independently of one another, our identification of MSNs endogenously expressing both D1R and D2R confirms that these cells are likely biologically relevant, with additional future work required to settle these controversies.

Compared to D1/2R MSNs, much less is known about D1/3R or D2/3R MSNs and their roles in striatal function. We identified D1/3R co-expression primarily in the NAc ventromedial shell and IC. Though the functional relevance of D1/3R MSNs has not been comprehensively studied, a limited number of studies suggest that D1/3R co-expression serves as a buffering mechanism to temper the stimulatory signaling by D1R and inhibitory signaling by D3R[50]. Such D1/3R signaling is relevant to levodopa-induced behavioral sensitization in hemiparkinsonian rodents and has been hypothesized to play a role in the actions of antipsychotic medications[50].

Our results show the OT as a region where D1/2R co-expressing MSNs are significantly enriched. To date, the functions of the OT and the IC within remain poorly understood. Important clues come from the OT's anatomy. As the most ventral striatal subregion, there are significant amounts

of dopaminergic signaling in the OT[51]. Moreover, D1R and D2R play opposing roles in functions mediated by OT, including in odor-conditioned reward responses[52]. We therefore hypothesize that D1/2R MSNs in the OT may represent a hybrid population producing responses intermediate between stimulatory $D1R^+$ and inhibitory $D2R^+$ MSNs. While D1/3R MSN function in the OT is unclear, D3R on its own is better characterized in this striatal subregion. OT $D3R^+$ MSNs are enriched in the IC and play a critical role in grooming behavior in mice[31]. Thus, D1/3R MSNs may also represent a hybrid population that produces phenotypes intermediate to D1R and D3R that integrate their respective opposing DA signaling.

To date, studies to dissect the respective roles of D1/2R and D1/3R subpopulations have been limited due to the inability to selectively target these subpopulations. Thus, most studies have been *in vitro*, relied on ectopic receptor overexpression, or on bacterial artificial chromosome (BAC) transgenic mice expressing fluorescent tags in $D1R^+$ versus $D2R^+$ MSNs, which has led to conflicting findings and unclear relevance in vivo[12, 29, 53]. The recent advent of intersectional genetic systems will facilitate future work to selectively dissect the functional relevance of co-expressing MSN subpopulations throughout the striatum.

3D mapping of D1R, D2R, and D3R expression across dorsal-ventral and rostral-caudal axes of the striatum revealed gradients of differential distribution for several MSN subpopulations, especially for co-expressing cells. This is best exemplified in D1/2R MSNs which exhibit a gradient of cell density which increases along the dorsal-ventral axis while decreasing along the rostral-caudal axis (Fig. 4). What is the relevance of such gradients? Gradients are well-established features of brain development, including the striatum[54]. Indeed, gradients of signaling by morphogens such as sonic hedgehog (Shh) and Wnts are critical for striatal development and dorsal-ventral patterning[54, 55]. These gradients may also persist throughout adulthood[56]. Therefore, we hypothesize that these patterns of co-expressing neurons represent echoes of earlier developmental programs, reflecting persistent morphogenic gradients that gave rise to these specific subpopulations originally.

Overall, our study provides a definitive characterization of DA receptor expression in adult mouse striatum. This reveals a much more heterogenous population of MSNs than previously appreciated and includes several distinct subpopulations of co-expressing striatal neurons. Our findings open the door to better understanding the functional relevance of these unique cell populations in the contexts of healthy and disease states.

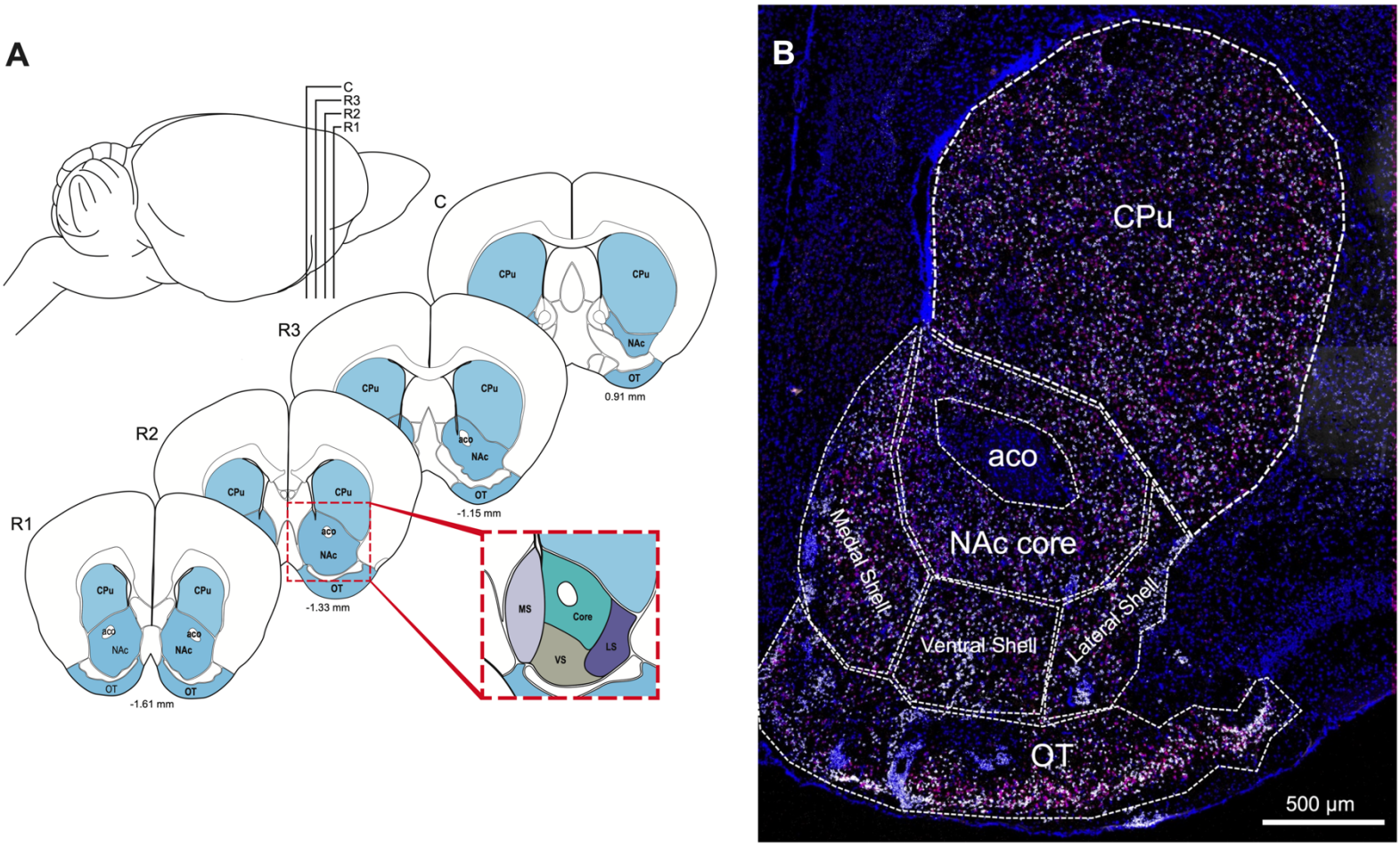

Figure 1. Diagrams representing the brain regions analyzed. (**A**) Coronal sections of mouse striatum were taken at Bregma -1.61 mm, referred to in the text and data as Rostral 1 (R1); -1.33 mm, Rostral 2 (R2); -1.15 mm, Rostral 3 (R3), and 0.91 mm, Caudal (C). The respective striatal subregions are annotated as follows: olfactory tubercle (OT), nucleus accumbens (NAc), anterior commissure (aco), as well as the caudate nucleus and putamen (CPu). The inset demonstrates the NAc subregions that were analyzed: NAc medial shell (MS), lateral shell (LS), ventral shell (VS), and core (see Supplementary Figs. S2, S3). (**B**) Annotation of a representative RNAscope image of mouse striatum displaying the striatal regions analyzed. Scale bar = 500 µm.

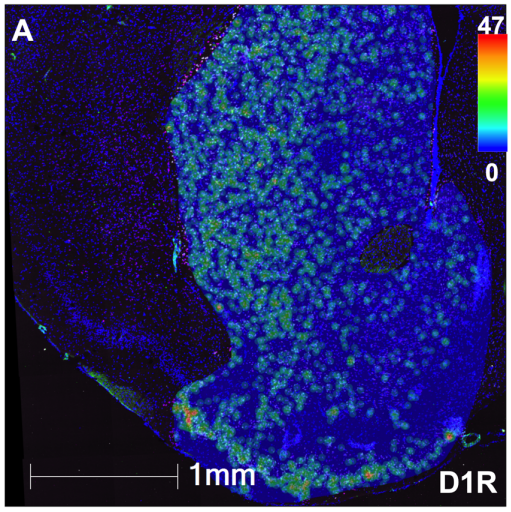

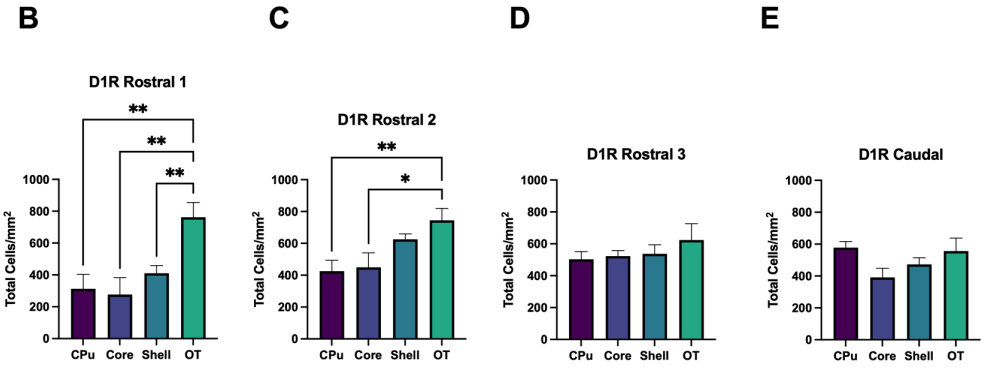

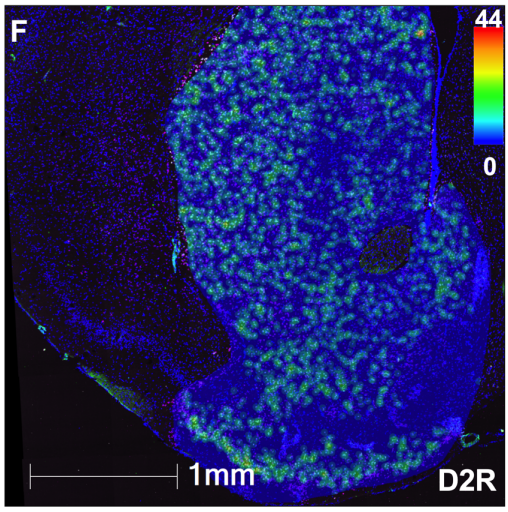

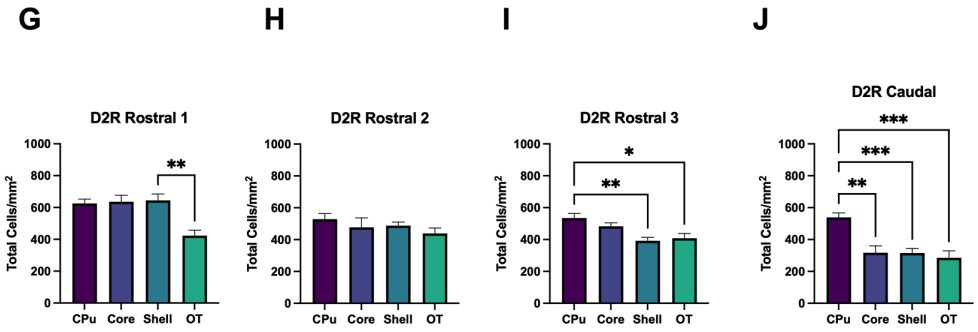

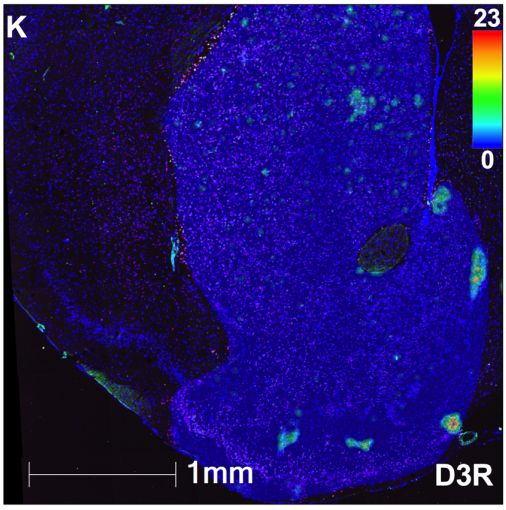

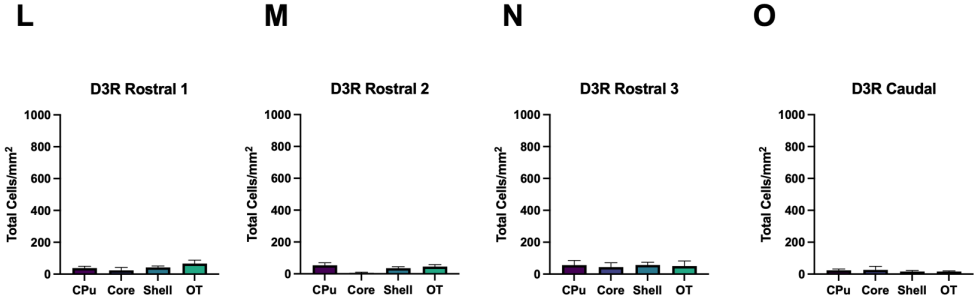

Figure 2. Spatial distribution of striatal dopamine D_1, D_2, and D_3 receptor expression in singly expressing neurons. Analyses of multiplex RNAscope data demonstrating dopamine D_1, D_2, and D_3 receptor expression in key striatal structures (CPu, Core, Shell, OT) along dorsal-ventral and rostral-caudal axes. (**A)** Representative heat map of the density of cells positive for D_1 receptor (D1R) expression in singly-expressing neurons, showing robust D1R expression throughout the striatum, particularly in the OT. (**B-E**) Quantification revealed a progressive decrease in OT enrichment of D1R-only cells in a rostral to caudal direction through the striatum. (**F**) Representative heat map showing a robust distribution of cells expressing dopamine D_2 receptor (D2R) mRNA throughout the striatum along the dorsal-ventral axis. **(G-J**) Quantitative analysis showed a steady decrease in the density of D2R-only neurons in the Shell and OT moving caudally (*p<0.05, **p<0.01, ***p<0.001), while remaining stable in the Core and CPu (p>0.05). (**K)** Representative heat map of MSNs expressing dopamine D_3 receptor (D3R) expression in striatal neurons. D3R expression was limited, aside from enrichment in selected subregions of the Shell and OT including within the Islands of Calleja (IC). (**L-O**) Quantitative analysis revealed uniformly low D3R expression in both dorsal-ventral and rostral-caudal directions (p>0.05). For **Panels A, F, and K**, scale bar = 1 mm; heat map legends represent the number of mRNA grains within a given cell. Mean ± SEM, n=6 mice for all conditions. *p<0.05, **p<0.01, ***p<0.001.

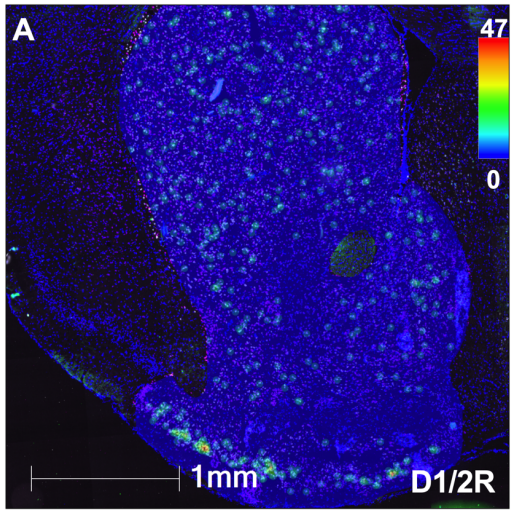

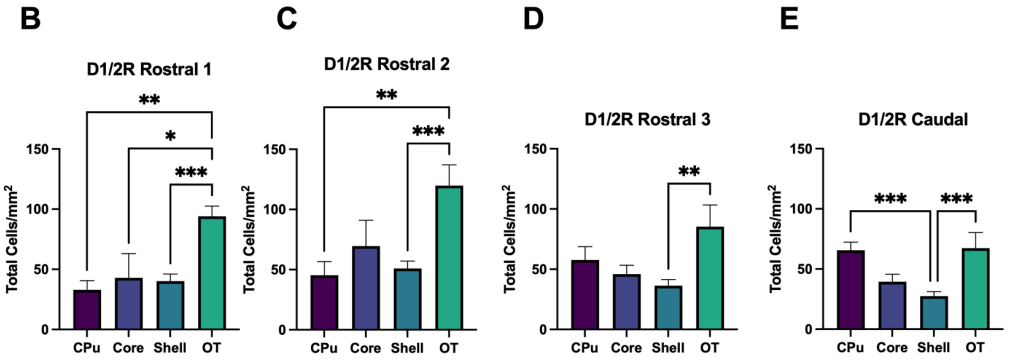

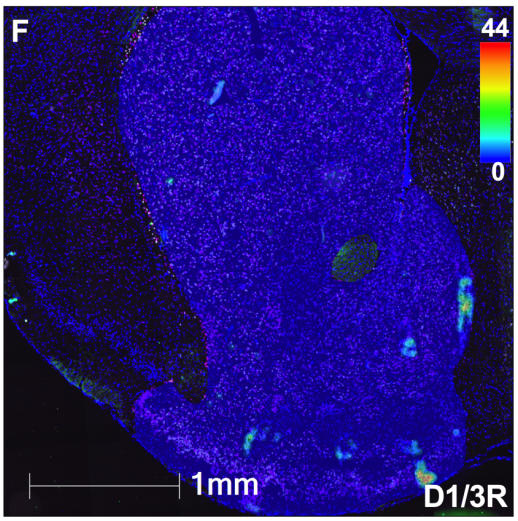

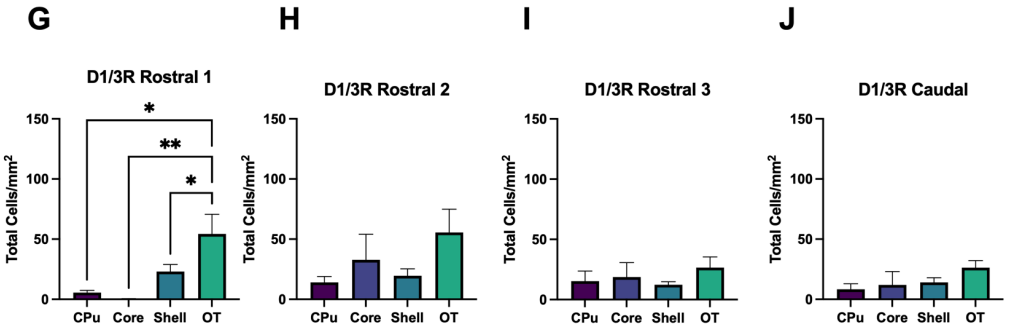

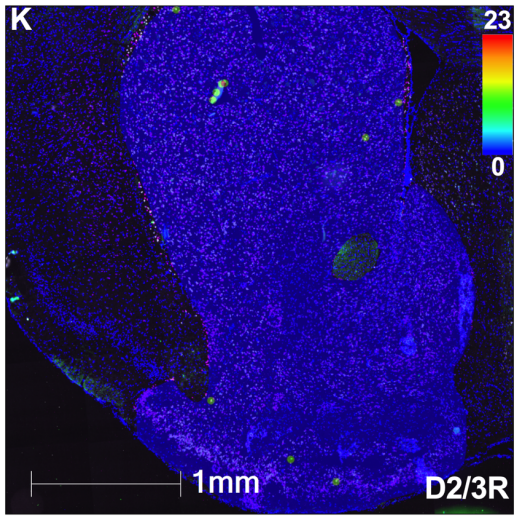

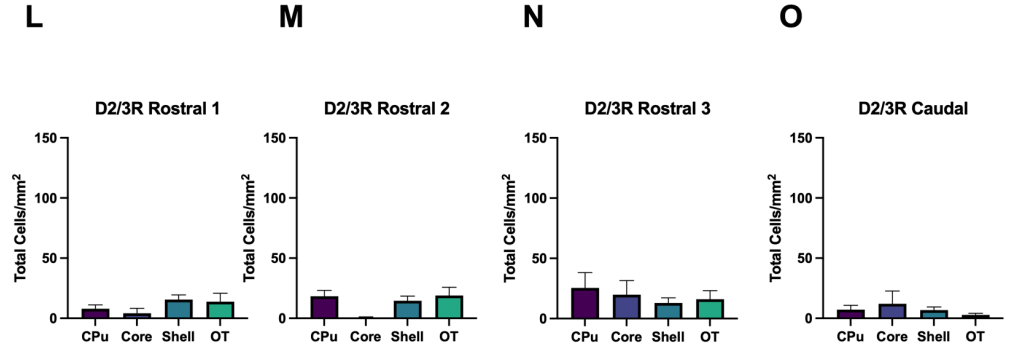

Figure 3. Spatial distribution of striatal dopamine D_1, D_2, or D_3 receptor expression in co-expressing neurons. (A) Representative heat map of MSNs co-expressing D1R/D2R (D1/2R). **(B-E)** Quantitation revealed that the highest density of D1/2R MSNs is in the OT. **(F)** Representative heat map showing the density of MSNs co-expressing D1R/D3R (D1/3R). **(G-J)** Quantitative analysis demonstrated preferential D1/3R co-expression in OT neurons that diminishes moving caudally (*p<0.05, **p<0.01). (**K**) Representative heat map of MSNs co-expressing D2R/D3R (D2/3R) revealed limited pockets of co-expression in the NAc and OT. **(L-O)** Quantitative analysis found low overall levels of D2/3R MSNs with no changes in distribution along dorsal-to-ventral or rostral-to-caudal axes (p>0.05). For **Panels A, F, and K**, scale bar = 1 mm; heat map legends represent the number of mRNA grains within a given cell. Mean ± SEM, n=6 mice for all conditions. *p<0.05, **p<0.01, ***p<0.001.

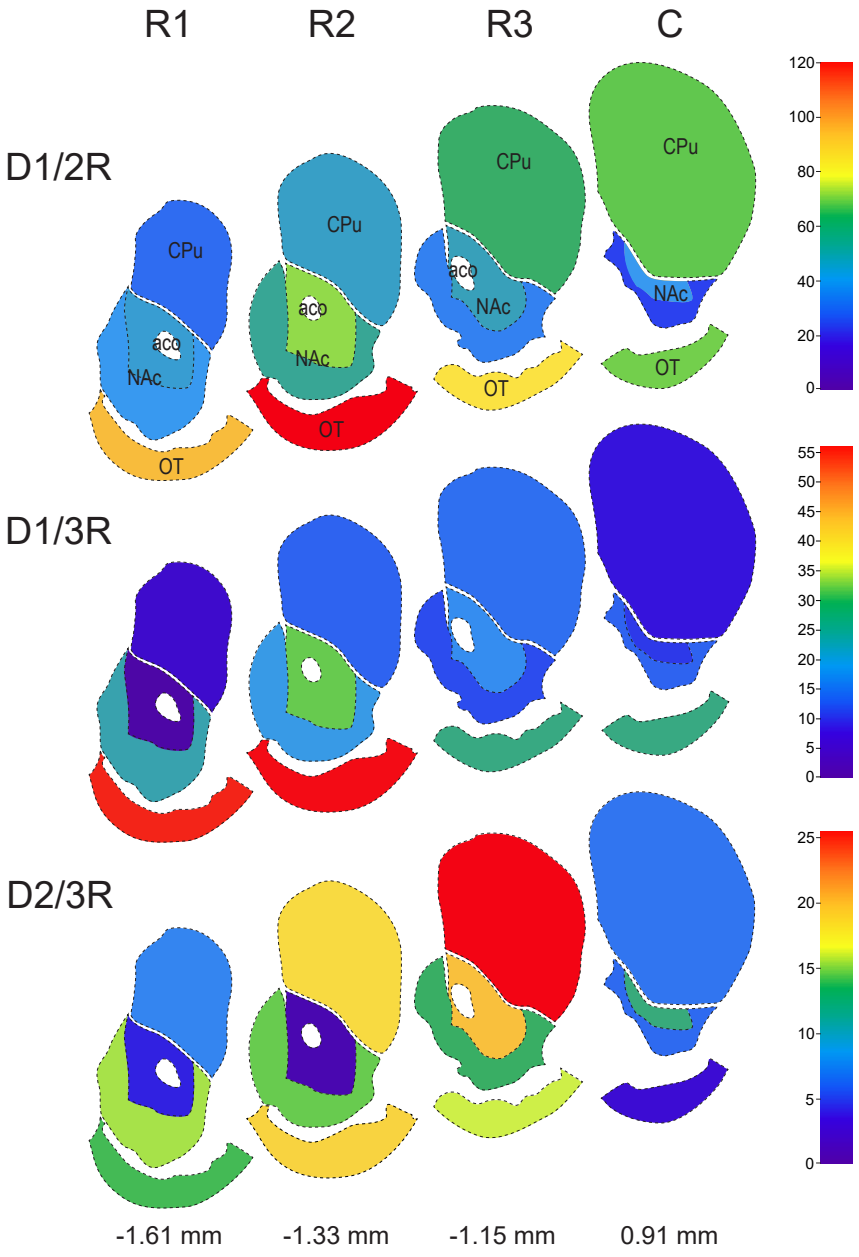

Figure 4. Schematic demonstrating 3D patterns of MSN DA receptor co-expression across dorsal-ventral and rostral-caudal axes. Distribution patterns of striatal MSNs co-expressing: D1R and D2R (D1/2R), D1R and D3R (D1/3R), or D2R and D3R (D2/3R) in the caudate putamen (CPu), nucleus accumbens (NAc), anterior commissure (aco), and olfactory tubercle (OT). Changes in density were also assessed across a rostral-caudal axis (R1 = -1.61mm, R2 = -1.33 mm, R3 = -1.15 mm, and C = 0.91 mm). The numbers on the scales represent the average positive cell density for each co-expressing receptor subpopulation.

Rostral 1	CPu	Core	Shell	OT
D1/D2+ out of total D1+ cells	10.6 ± 1.5	8.2 ± 2.5	9.3 ± 1.0	14.8 ± 1.4
D1/D2+ out of total D2+ cells	6.7 ± 1.9	6.0 ± 2.2	6.5 ± 0.8	21.2 ± 2.2
D1/D3 out of D1+ cells	2.2± 0.9	0.0 ± 0.0	7.0 ± 1.9	7.4 ± 2.3
D2/D3+ out of D2+ cells	1.2 ± 0.5	0.0 ± 0.0	1.9 ± 0.5	5.0 ± 2.1

Table 1.1: Percentage of striatal medium spiny neurons that co-express dopamine receptors in rostral 1 section (Bregma-1.61mm)

Rostral 2	CPu	Core	Shell	OT
D1/D2+ out of D1+ cells	11.6 ± 1.8	10.8 ± 2.7	8.2 ± 0.7	15.5 ± 1.5
D1/D2+ out of D2+ cells	8.0 ± 1.7	10.4 ± 2.9	10.2 ± 1.0	28.1 ± 3.9
D1/D3 out of D1+ cells	3.3 ± 0.9	0.1 ± 0.1	1.9 ± 0.4	7.1 ± 1.8
D2/D3+ out of D2+ cells	3.8 ± 1.1	0.0 ± 0.0	1.8 ± 0.5	2.7 ± 0.8

Table 1.2: Percentage of striatal medium spiny neurons that co-express dopamine receptors in rostral 2 section (Bregma -1.33mm)

Rostral 3	CPu	Core	Shell	OT
D1/D2+ out of D1+ cells	10.6 ± 1.2	8.8 ± 1.1	6.4 ± 0.6	12.9 ± 1.3
D1/D2+ out of D2+ cells	10.3 ± 1.7	9.5 ± 1.4	8.4 ± 1.0	19.9 ± 3.9
D1/D3 out of D1+ cells	0.8 ± 0.4	0.0 ± 0.0	1.2 ± 0.3	3.6 ± 1.1
D2/D3+ out of D2+ cells	1.6± 0.9	0.2 ± 0.2	1.2 ± 0.5	2.6 ± 1.1

Table 1.3: Percentage of striatal medium spiny neurons that co-express dopamine receptors in rostral 3 section (Bregma -1.15mm)

Caudal	CPu	Core	Shell	OT
D1/D2+ out of D1+ cells	11.3 ± 0.8	10.9 ± 2.3	5.7 ± 0.8	11.9 ± 2.2
D1/D2+ out of D2+ cells	11.9 ± 0.9	12.8 ± 2.0	8.9 ± 1.1	26.0 ± 5.7
D1/D3 out of D1+ cells	0.8 ± 0.3	0.1 ± 0.1	2.1 ± 0.6	3.9 ± 0.8
D2/D3+ out of D2+ cells	0.4 ± 0.2	0.0± 0.0	0.0± 0.0	0.2 ± 0.2

Table 1.4: Percentage of striatal medium spiny neurons that co-express dopamine receptors in the caudal section (Bregma +0.91mm)

Table 1. Percentage of dopamine D_1, D_2, and D_3 receptors co-expressed in D_1^+ and D_2^+ MSNs across ventral-dorsal and rostral-caudal axes.

References

1. Volkow ND, Wang GJ, Fowler JS, Tomasi D, Telang F, Baler R. Addiction: decreased reward sensitivity and increased expectation sensitivity conspire to overwhelm the brain's control circuit. BioEssays : news and reviews in molecular, cellular and developmental biology. 2010;32(9):748-55. Epub 2010/08/24. doi: 10.1002/bies.201000042. PubMed PMID: 20730946; PMCID: PMC2948245.

2. Calabresi P, Picconi B, Tozzi A, Ghiglieri V, Di Filippo M. Direct and indirect pathways of basal ganglia: a critical reappraisal. Nat Neurosci. 2014;17(8):1022-30. Epub 20140728. doi: 10.1038/nn.3743. PubMed PMID: 25065439.

3. Beaulieu JM, Espinoza S, Gainetdinov RR. Dopamine receptors - IUPHAR Review 13. British journal of pharmacology. 2015;172(1):1-23. Epub 2015/02/12. doi: 10.1111/bph.12906. PubMed PMID: 25671228; PMCID: PMC4280963.

4. Cepeda C, André VM, Yamazaki I, Wu N, Kleiman-Weiner M, Levine MS. Differential electrophysiological properties of dopamine D1 and D2 receptor-containing striatal medium-sized spiny neurons. The European journal of neuroscience. 2008;27(3):671-82. doi: 10.1111/j.1460-9568.2008.06038.x. PubMed PMID: 18279319.

5. Allichon MC, Ortiz V, Pousinha P, Andrianarivelo A, Petitbon A, Heck N, Trifilieff P, Barik J, Vanhoutte P. Cell-Type-Specific Adaptions in Striatal Medium-Sized Spiny Neurons and Their Roles in Behavioral Responses to Drugs of Abuse. Frontiers in synaptic neuroscience. 2021;13:799274. Epub 20211214. doi: 10.3389/fnsyn.2021.799274. PubMed PMID: 34970134; PMCID: PMC8712310.

6. Strickland JC, Gipson CD, Dunn KE. Dopamine Supersensitivity: A Novel Hypothesis of Opioid-Induced Neurobiological Mechanisms Underlying Opioid-Stimulant Co-use and Opioid Relapse. Frontiers in psychiatry. 2022;13. doi: 10.3389/fpsyt.2022.835816.

7. Soares-Cunha C, Coimbra B, Sousa N, Rodrigues AJ. Reappraising striatal D1- and D2-neurons in reward and aversion. Neurosci Biobehav Rev. 2016;68:370-86. Epub 20160524. doi: 10.1016/j.neubiorev.2016.05.021. PubMed PMID: 27235078.

8. Surmeier DJ, Ding J, Day M, Wang Z, Shen W. D1 and D2 dopamine-receptor modulation of striatal glutamatergic signaling in striatal medium spiny neurons. Trends Neurosci. 2007;30(5):228-35. Epub 20070403. doi: 10.1016/j.tins.2007.03.008. PubMed PMID: 17408758.

9. Ren K, Guo B, Dai C, Yao H, Sun T, Liu X, Bai Z, Wang W, Wu S. Striatal Distribution and Cytoarchitecture of Dopamine Receptor Subtype 1 and 2: Evidence from Double-Labeling Transgenic Mice. Frontiers in neural circuits. 2017;11:57. Epub 20170817. doi: 10.3389/fncir.2017.00057. PubMed PMID: 28860974; PMCID: PMC5562971.

10. Martel JC, Gatti McArthur S. Dopamine Receptor Subtypes, Physiology and Pharmacology: New Ligands and Concepts in Schizophrenia. Frontiers in pharmacology. 2020;11:1003. Epub 20200714. doi: 10.3389/fphar.2020.01003. PubMed PMID: 32765257; PMCID: PMC7379027.

11. Enoksson T, Bertan-Gonzalez, J., & Christie, M.J. Nucleus accumbens D2- and D1-receptor expressing medium spiny neurons are selectively activated by morphine withdrawal and acute morphine, respectively. Neuropharmacology. 2012;62(8):2463-71. doi: 10.1016/j.neuropharm.2012.02.020.

12. Hearing MC, Jedynak, J., Ebner, S.R., Ingebretson, A., Asp., A. J., Fischer, R.A., Schmidt, C., Larson, E.B., & Thomas, M.J. . Reversal of morphine-induced cell-type-specific synaptic plasticity in the nucleus accumbens shell blocks reinstatement Proceedings of the National Academy of Sciences. 2016;113(3):757-62. doi: 10.1073/pnas.1519248113.

13. Graziane NM, Sun, S., Wright, W.J., Jang, D., Liu, Z., Huang Y.H., Nestler, E.J., Wang, Y. T., Schlüter, O.M., & Dong, Y. . Opposing mechanisms mediate morphine- and cocaine- induced generation of silent synapses. Nature Neuroscience. 2016;19(7):915-25. doi: 10.1038/nn.4313

14. McDevitt DS, Jonik, B., & Graziane, N.M. . Morphine differentially alters the synaptic and intrinsic properties of D1R- and D2R-expressing medium spiny neurons in the nucleus accumbens. Fronters in Synaptic Neuroscience. 2019;11. doi: 10.3389/fnsyn.2019.00035

15. Robertson GS, Jian M. D1 and D2 dopamine receptors differentially increase Fos-like immunoreactivity in accumbal projections to the ventral pallidum and midbrain. Neuroscience. 1995;64(4):1019-34. doi: 10.1016/0306-4522(94)00426-6. PubMed PMID: 7753373.

16. Stephenson-Jones M, Bravo-Rivera C, Ahrens S, Furlan A, Xiao X, Fernandes-Henriques C, Li B. Opposing Contributions of GABAergic and Glutamatergic Ventral Pallidal Neurons to Motivational Behaviors. Neuron. 2020;105(5):921-33.e5. Epub 20200113. doi: 10.1016/j.neuron.2019.12.006. PubMed PMID: 31948733; PMCID: PMC8573387.

17. Calipari ES, Bagot RC, Purushothaman I, Davidson TJ, Yorgason JT, Peña CJ, Walker DM, Pirpinias ST, Guise KG, Ramakrishnan C, Deisseroth K, Nestler EJ. In vivo imaging identifies temporal signature of D1 and D2 medium spiny neurons in cocaine reward. Proc Natl Acad Sci U S A. 2016;113(10):2726-31. Epub 20160201. doi: 10.1073/pnas.1521238113. PubMed PMID: 26831103; PMCID: PMC4791010.

18. Lobo MK, Covington HE, 3rd, Chaudhury D, Friedman AK, Sun H, Damez-Werno D, Dietz DM, Zaman S, Koo JW, Kennedy PJ, Mouzon E, Mogri M, Neve RL, Deisseroth K, Han MH, Nestler EJ. Cell type-specific loss of BDNF signaling mimics optogenetic control of cocaine

reward. Science. 2010;330(6002):385-90. doi: 10.1126/science.1188472. PubMed PMID: 20947769; PMCID: PMC3011229.

19. Kupchik YM, Brown RM, Heinsbroek JA, Lobo MK, Schwartz DJ, Kalivas PW. Coding the direct/indirect pathways by D1 and D2 receptors is not valid for accumbens projections. Nat Neurosci. 2015;18(9):1230-2. Epub 2015/07/28. doi: 10.1038/nn.4068. PubMed PMID: 26214370; PMCID: PMC4551610.

20. Smith RJ, Lobo MK, Spencer S, Kalivas PW. Cocaine-induced adaptations in D1 and D2 accumbens projection neurons (a dichotomy not necessarily synonymous with direct and indirect pathways). Curr Opin Neurobiol. 2013;23(4):546-52. Epub 20130218. doi: 10.1016/j.conb.2013.01.026. PubMed PMID: 23428656; PMCID: PMC3681928.

21. Fenu S, Spina, L., Rivas, E., Longoni, R., & Di Chiara, G. Morphine-conditioned single-trial place preference: role of nulceus accumbens shell dopamine receptors in acquisition, but not expression. Psychopharmacology. 2006;187:143-53. doi: https://doi.org/10.1007/s00213-006-0415-2.

22. Manzanedo C, Aguilar, M., Rodríguez-Arias, M., & Miñarro, J. Effects of dopamine antagonists with different receptor blockade profiles on morphine-induced place preference in male mice. Behavioural Brain Research. 2001;121(1-2):189-97. doi: https://doi.org/10.1016/S0166-4328(01)00164-4.

23. Wong AC, Shetreat ME, Clarke JO, Rayport S. D1- and D2-like dopamine receptors are co-localized on the presynaptic varicosities of striatal and nucleus accumbens neurons in vitro. Neuroscience. 1999;89(1):221-33. doi: 10.1016/s0306-4522(98)00284-x. PubMed PMID: 10051231.

24. Bonnavion P, Varin C, Fakhfouri G, De Groote A, Cornil A, Isingrini E, Rainer Q, Xu K, Tzavara E, Vigneault E, Dumas S, de Kerchove d'Exaerde A, Giros B. Unexpected inhibition of motor function by dopamine activation of D1/D2 co-expressing striatal neurons. bioRxiv. 2022:2022.04.05.487163. doi: 10.1101/2022.04.05.487163.

25. Thibault D, Loustalot F, Fortin GM, Bourque MJ, Trudeau L. Evaluation of D1 and D2 dopamine receptor segregation in the developing striatum using BAC transgenic mice. PLoS One. 2013;8(7):e67219. Epub 20130702. doi: 10.1371/journal.pone.0067219. PubMed PMID: 23843993; PMCID: PMC3699584.

26. Aizman O, Brismar H, Uhlén P, Zettergren E, Levey AI, Forssberg H, Greengard P, Aperia A. Anatomical and physiological evidence for D1 and D2 dopamine receptor colocalization in neostriatal neurons. Nat Neurosci. 2000;3(3):226-30. doi: 10.1038/72929. PubMed PMID: 10700253.

27. Perreault ML, Hasbi A, Alijaniaram M, Fan T, Varghese G, Fletcher PJ, Seeman P, O'Dowd BF, George SR. The dopamine D1-D2 receptor heteromer localizes in dynorphin/enkephalin neurons: increased high affinity state following amphetamine and in schizophrenia. J Biol Chem. 2010;285(47):36625-34. Epub 2010/09/25. doi: 10.1074/jbc.M110.159954. PubMed PMID: 20864528; PMCID: PMC2978591.

28. Perreault ML, Hasbi A, O'Dowd BF, George SR. Heteromeric dopamine receptor signaling complexes: emerging neurobiology and disease relevance. Neuropsychopharmacology. 2014;39(1):156-68. Epub 2013/06/19. doi: 10.1038/npp.2013.148. PubMed PMID: 23774533; PMCID: PMC3857642.

29. Frederick AL, Yano H, Trifilieff P, Vishwasrao HD, Biezonski D, Mészáros J, Urizar E, Sibley DR, Kellendonk C, Sonntag KC, Graham DL, Colbran RJ, Stanwood GD, Javitch JA. Evidence against dopamine D1/D2 receptor heteromers. Mol Psychiatry. 2015;20(11):1373-85. Epub 20150106. doi: 10.1038/mp.2014.166. PubMed PMID: 25560761; PMCID: PMC4492915.

30. Booze RM, Wallace DR. Dopamine D2 and D3 receptors in the rat striatum and nucleus accumbens: use of 7-OH-DPAT and [125I]-iodosulpride. Synapse. 1995;19(1):1-13. doi: 10.1002/syn.890190102. PubMed PMID: 7709338.

31. Zhang YF, Vargas Cifuentes L, Wright KN, Bhattarai JP, Mohrhardt J, Fleck D, Janke E, Jiang C, Cranfill SL, Goldstein N, Schreck M, Moberly AH, Yu Y, Arenkiel BR, Betley JN, Luo W, Stegmaier J, Wesson DW, Spehr M, Fuccillo MV, Ma M. Ventral striatal islands of Calleja neurons control grooming in mice. Nat Neurosci. 2021;24(12):1699-710. Epub 20211118. doi: 10.1038/s41593-021-00952-z. PubMed PMID: 34795450; PMCID: PMC8639805.

32. Sokoloff P, Diaz J, Le Foll B, Guillin O, Leriche L, Bezard E, Gross C. The dopamine D3 receptor: a therapeutic target for the treatment of neuropsychiatric disorders. CNS Neurol Disord Drug Targets. 2006;5(1):25-43. doi: 10.2174/187152706784111551. PubMed PMID: 16613552.

33. Marcellino D, Ferre S, Casado V, Cortes A, Le Foll B, Mazzola C, Drago F, Saur O, Stark H, Soriano A, Barnes C, Goldberg SR, Lluis C, Fuxe K, Franco R. Identification of dopamine D1-D3 receptor heteromers. Indications for a role of synergistic D1-D3 receptor interactions in the striatum. J Biol Chem. 2008;283(38):26016-25. Epub 2008/07/23. doi: 10.1074/jbc.M710349200. PubMed PMID: 18644790; PMCID: PMC2533781.

34. Fiorentini C, Busi C, Gorruso E, Gotti C, Spano P, Missale C. Reciprocal regulation of dopamine D1 and D3 receptor function and trafficking by heterodimerization. Mol Pharmacol. 2008;74(1):59-69. Epub 20080418. doi: 10.1124/mol.107.043885. PubMed PMID: 18424554.

35. Palacios JM, Camps M, Cortés R, Probst A. Mapping dopamine receptors in the human brain. J Neural Transm Suppl. 1988;27:227-35. doi: 10.1007/978-3-7091-8954-2_20. PubMed PMID: 2969952.

36. Buck SA, Steinkellner T, Aslanoglou D, Villeneuve M, Bhatte SH, Childers VC, Rubin SA, De Miranda BR, O'Leary EI, Neureiter EG, Fogle KJ, Palladino MJ, Logan RW, Glausier JR, Fish KN, Lewis DA, Greenamyre JT, McCabe BD, Cheetham CEJ, Hnasko TS, Freyberg Z. Vesicular glutamate transporter modulates sex differences in dopamine neuron vulnerability to age-related neurodegeneration. Aging cell. 2021:e13365. Epub 2021/04/29. doi: 10.1111/acel.13365. PubMed PMID: 33909313.

37. Balasubramani PP, Chakravarthy VS, Ravindran B, Moustafa AA. A network model of basal ganglia for understanding the roles of dopamine and serotonin in reward-punishment-risk based decision making. Front Comput Neurosci. 2015;9:76. Epub 20150617. doi: 10.3389/fncom.2015.00076. PubMed PMID: 26136679; PMCID: PMC4469836.

38. Bonnavion P, Varin C, Fakhfouri G, Olondo PM, Groote AD, Cornil A, Lopez RL, Fernandez EP, Isingrini E, Rainer Q, Xu K, Tzavara E, Vigneault E, Dumas S, d'Exaerde AdK, Giros B. Unexpected contributions of striatal projection neurons coexpressing dopamine D1 and D2 receptors in balancing motor control. bioRxiv. 2023:2022.04.05.487163. doi: 10.1101/2022.04.05.487163.

39. Kreitzer AC. Physiology and pharmacology of striatal neurons. Annu Rev Neurosci. 2009;32:127-47. doi: 10.1146/annurev.neuro.051508.135422. PubMed PMID: 19400717.

40. Brundage JN, Mason CP, Wadsworth HA, Finuf CS, Nelson JJ, Ronström PJW, Jones SR, Siciliano CA, Steffensen SC, Yorgason JT. Regional and sex differences in spontaneous striatal dopamine transmission. J Neurochem. 2022;160(6):598-612. Epub 20210816. doi: 10.1111/jnc.15473. PubMed PMID: 34265080.

41. Seppä T, Ahtee L. Comparison of the effects of epibatidine and nicotine on the output of dopamine in the dorsal and ventral striatum of freely-moving rats. Naunyn Schmiedebergs Arch Pharmacol. 2000;362(4-5):444-7. doi: 10.1007/s002100000324. PubMed PMID: 11111841.

42. See RE, Elliott JC, Feltenstein MW. The role of dorsal vs ventral striatal pathways in cocaine-seeking behavior after prolonged abstinence in rats. Psychopharmacology (Berl). 2007;194(3):321-31. Epub 20070624. doi: 10.1007/s00213-007-0850-8. PubMed PMID: 17589830.

43. Stanley G, Gokce O, Malenka RC, Südhof TC, Quake SR. Continuous and Discrete Neuron Types of the Adult Murine Striatum. Neuron. 2020;105(4):688-99.e8. Epub 20191205. doi: 10.1016/j.neuron.2019.11.004. PubMed PMID: 31813651.

44. Gagnon D, Petryszyn S, Sanchez MG, Bories C, Beaulieu JM, De Koninck Y, Parent A, Parent M. Striatal Neurons Expressing D(1) and D(2) Receptors are Morphologically Distinct and Differently Affected by Dopamine Denervation in Mice. Sci Rep. 2017;7:41432. Epub 20170127. doi: 10.1038/srep41432. PubMed PMID: 28128287; PMCID: PMC5269744.

45. George SR, Kern A, Smith RG, Franco R. Dopamine receptor heteromeric complexes and their emerging functions. Prog Brain Res. 2014;211:183-200. doi: 10.1016/b978-0-444-63425-2.00008-8. PubMed PMID: 24968781.

46. Rashid AJ, So CH, Kong MM, Furtak T, El-Ghundi M, Cheng R, O'Dowd BF, George SR. D1-D2 dopamine receptor heterooligomers with unique pharmacology are coupled to rapid activation of Gq/11 in the striatum. Proc Natl Acad Sci U S A. 2007;104(2):654-9. Epub 20061228. doi: 10.1073/pnas.0604049104. PubMed PMID: 17194762; PMCID: PMC1766439.

47. Perreault ML, Hasbi A, Shen MYF, Fan T, Navarro G, Fletcher PJ, Franco R, Lanciego JL, George SR. Disruption of a dopamine receptor complex amplifies the actions of cocaine. Eur Neuropsychopharmacol. 2016;26(9):1366-77. Epub 20160730. doi: 10.1016/j.euroneuro.2016.07.008. PubMed PMID: 27480020.

48. Hasbi A, Nguyen T, Rahal H, Manduca JD, Miksys S, Tyndale RF, Madras BK, Perreault ML, George SR. Sex difference in dopamine D1-D2 receptor complex expression and signaling affects depression- and anxiety-like behaviors. Biol Sex Differ. 2020;11(1):8. Epub 20200222. doi: 10.1186/s13293-020-00285-9. PubMed PMID: 32087746; PMCID: PMC7035642.

49. Uefune F, Aonishi T, Kitaguchi T, Takahashi H, Seino S, Sakano D, Kume S. Dopamine Negatively Regulates Insulin Secretion Through Activation of D1-D2 Receptor Heteromer. Diabetes. 2022;71(9):1946-61. doi: 10.2337/db21-0644. PubMed PMID: 35728809.

50. Schwartz JC, Diaz J, Bordet R, Griffon N, Perachon S, Pilon C, Ridray S, Sokoloff P. Functional implications of multiple dopamine receptor subtypes: the D1/D3 receptor coexistence. Brain Res Brain Res Rev. 1998;26(2-3):236-42. doi: 10.1016/s0165-0173(97)00046-5. PubMed PMID: 9651537.

51. Murata K, Kanno M, Ieki N, Mori K, Yamaguchi M. Mapping of Learned Odor-Induced Motivated Behaviors in the Mouse Olfactory Tubercle. J Neurosci. 2015;35(29):10581-99. doi: 10.1523/jneurosci.0073-15.2015. PubMed PMID: 26203152; PMCID: PMC6605114.

52. Gadziola MA, Stetzik LA, Wright KN, Milton AJ, Arakawa K, Del Mar Cortijo M, Wesson DW. A Neural System that Represents the Association of Odors with Rewarded Outcomes and Promotes Behavioral Engagement. Cell Rep. 2020;32(3):107919. doi: 10.1016/j.celrep.2020.107919. PubMed PMID: 32697986; PMCID: PMC7470245.

53. Lee SP, So, C.H., Rashid, A.J., Varghese, G., Cheng R., Lanca, A.J., O'Dowd, B.F., & George, S.R. Dopamine D1 and D2 receptor co-activation generates a novel phospholipase C-mediated calcium signal. Journal of Biological Chemistry. 2004;279(34):35671-8. doi: 10.1074/jbc.m401923200.

54. Evans AE, Kelly CM, Precious SV, Rosser AE. Molecular regulation of striatal development: a review. Anat Res Int. 2012;2012:106529. Epub 20120126. doi: 10.1155/2012/106529. PubMed PMID: 22567304; PMCID: PMC3335634.

55. Fuccillo M, Rallu M, McMahon AP, Fishell G. Temporal requirement for hedgehog signaling in ventral telencephalic patterning. Development. 2004;131(20):5031-40. Epub 20040915. doi: 10.1242/dev.01349. PubMed PMID: 15371303.

56. Ihrie RA, Shah JK, Harwell CC, Levine JH, Guinto CD, Lezameta M, Kriegstein AR, Alvarez-Buylla A. Persistent sonic hedgehog signaling in adult brain determines neural stem cell positional identity. Neuron. 2011;71(2):250-62. doi: 10.1016/j.neuron.2011.05.018. PubMed PMID: 21791285; PMCID: PMC3346180.

Acknowledgments

We sincerely thank Mary Brady for assistance with figure design as well as Dr. Alan Watson, Dr. Simon Watkins and the Center for Biologic Imaging at the University of Pittsburgh for help and support with imaging and image processing. This work was supported by NIH grants R01ES034037 (ZF), R21AG068607 (ZF), R21DA052419 (RWL, ZF), R21AA028800 (RWL, ZF).

Author Contributions

Design of the work (JG, SP, ZF); Acquisition, analysis, or interpretation of data for the work (JG, SP, CS, SAB, MCG, JRG, HAT, YD, ARP, RWL, ZF); Writing of the initial manuscript draft (JG, ZF) with other authors contributing to subsequent writing and editing.

Competing Interests

The authors declare no competing interests.